Developing a microfluidic-based system to quantify cell capture efficiency

YANG Fan, GAO YuXin, ZHANG Yan, CHEN Juan & LONG Mian[†]

National Microgravity Laboratory and Center for Biomechanics and Bioengineering, Institute of Mechanics, Chinese Academy of Sciences, Beijing 100080, China

Micro-fabrication technology has substantial potential for identifying molecular markers expressed on the surfaces of tissue cells and viruses. It has been found in several conceptual prototypes that cells with such markers are able to be captured by their antibodies immobilized on microchannel substrates and unbound cells are flushed out by a driven flow. The feasibility and reliability of such a microfluidic-based assay, however, remains to be further tested. In the current work, we developed a microfluidic-based system consisting of a microfluidic chip, an image grabbing unit, data acquisition and analysis software, as well as a supporting base. Specific binding of CD59-expressed or BSA-coupled human red blood cells (RBCs) to anti-CD59 or anti-BSA antibody-immobilized chip surfaces was quantified by capture efficiency and by the fraction of bound cells. Impacts of respective flow rate, cell concentration, antibody concentration and site density were tested systematically. The measured data indicated that the assay was robust. The robustness was further confirmed by capture efficiencies measured from an independent ELISA-based cell binding assay. These results demonstrated that the system developed provided a new platform to effectively quantify cellular surface markers effectively, which promoted the potential applications in both biological studies and clinical diagnoses.

Cell surface molecules usually serve as markers in many biological processes. They are also crucial for clinical diagnosis and prognosis because the expression of different surface markers is often related to various types of diseases[1]. In some cases, identifying the expression of surface markers has even become an indispensable step[2]. Among developed techniques in this sense, fluorescence-activated cell sorting or the flow cytometry (FACS) technique may be the most widely-applicable assay for cell-surface marker determination. Using FACS, the variety and amount of marker molecules are able to be quantified using fluorescence intensity of dye-labeled anti-marker antibodies bound specifically to cell surface markers[3,4]. However, as a highly-integrated technique, FACS appears to be expensive, time-consuming, and low-throughout, which confines further applications due to high cost, bulky size, and the requirement for trained specialists. Enzyme-linked immu-

nosorbent assay (ELISA)-based cell binding assay is an alternative method to identify surface markers on cell or virus surfaces[5]. It is a simple and well-defined assay and widely used in laboratories it is still time-consuming to quantify the expression and functionality of surface markers in low-throughout analysis with manual operations.

Recent progress in micro-fabrication technology provides alternative possibility for mapping surface makers. For example, antibody microarray chips have demonstrated great potential in cell phenotyping and disease diagnosis by identifying surface markers, in which

marker molecule-expressed cells are captured by anti-marker antibodies immobilized onto a nitrocellulose film or a glass slide. Acquired cell capture efficiency or binding density reports a qualitative or semi-quantitative determination for cell-surface markers[6–10]. Thus, microarray chips serve as a platform for rapidly screening cell surface markers at high-throughout analysis with much lower cost as compared to FACS. Like other microarray techniques[11], however, antibody microarrays lack robustness and reproducibility[12,13]. For example, removing unbound cells is performed manually[6,7,9,10]. This shortcoming, combined with other uncertainties such as non-specific bindings, time-dependent variation of maker molecule expression, and unavoidable false-positive or false-negative signals, biases the measured capture efficiency or binding density[6]. Thus, a well-controlled experimental procedure, automatic data acquisition, and quantitative data analysis are required for establishing a commercial antibody microarray.

One possible solution to partially address the above issues may be microfluidic techniques. In addition to taking the advantage of substantially reducing the volume of sample and probe in micro- or nanoliters using microchannels in dimensions of tens to hundreds of micrometers, this technique also achieves very well high-throughout measurements and automatic data analysis yielding more accurate data in a much shorter period[14,15]. Over the recent decades, it was also extensively used in immunoassays[16,17], such as developing a microfluidic-based ELISA to identify soluble antigens by immobilized antibodies on substrates[18–21]. In addition, some groups have integrated microfabrication technology with FACS for a cell sorter which is positive for quantifying cell-surface markers in microfluidic chips[22,23]. However, these are techniques requiring fluorescent labeling. Only a few investigations have identified surface markers using microfluidic-based label-free assays. For example, a conceptual microfluidic-based portable prototype has been developed for identifying cell-surface markers, in which an antibody-immobilized microfluidic chip is used to automatically wash unbound cells out with a driven flow and then to effectively capture antigen-expressed cells[24,25]. The regulating mechanism that the cell capture mechanism mediated by binding surface markers to their counterpart molecules, is affected by flow dynamics as well as by cellular concentration and molecular expression. However, it needs to be further understood prior to

developing a commercialized microfluidic-based system.

Here we developed a microfluidic-based system to identify surface markers expressed or coupled on human red blood cells (RBCs). By integrating the micro-fabrication technique with biological measurements, microfluidic manipulation, and data acquisition and analysis, the system was enabled to quantify the capture efficiency of antigen- or receptor-expressed cells to antibody- or ligand-immobilized chip surfaces. Two molecular systems were used to test the system: one was the CD59 antigen constitutively expressed on RBCs[26], and the other was bovine serum albumin (BSA) reconstructed on the RBC surface[3,4,27–29]. Impacts of flow rate, cell concentration, antibody concentration and site density were quantified by comparing the capture efficiencies of bound RBCs.

1 Experimental procedures

1.1 Cells, proteins and reagents

Human RBCs were isolated from fresh whole blood of healthy donors, and washed three times in phosphate buffer solution (PBS, pH 7.4). Collected RBCs were re-suspended and used to couple the proteins of interest onto their surfaces. Plain or protein-coupled RBCs were then used to measure their capture on chip surfaces.

BSA proteins, anti-BSA and anti-CD59 monoclonal antibodies (mAbs) (all mouse IgG1), FITC-conjugated goat-anti-mouse secondary antibody, as well as bovine casein, were purchased from Sigma (USA). 3-Aminopropyltriethoxysilane (APTES), N-hydroxysuccinimide (NHS), 1-ethyl-3-(3-dimethylaminopropyl) carbodiimide hydrochloride (EDC), and sulfosuccinimidyl-6- (biotin-amido) hexanoate (Sulfo-NHS-LC-Biotin) were purchased from Pierce (France). Poly(dimethylsiloxane) (PDMS) was from Dow Corning (USA), and horseradish peroxidase streptavidin was from Vector (USA).

1.2 Microfluidic chip fabrication

Microfluidic chip with a channel of 100 μm×50 μm (width×height) was fabricated using a modified rapid prototyping protocol[30,31]. Briefly, fluidic channels were replicated into a thin layer of SU-8 photoresist deposited on a silicon substrate by a photomask exposed to UV light. Curing reagent and PDMS pre-polymer were thoroughly mixed in a ratio of 1∶10. The pre-polymer mixture was degassed using a vacuum pump at 13.33 Pa in a desiccator for 1 h to remove air bulbs onto a master

mold, and cured at 80℃ for 1 h in an oven. After curing, PDMS replicas were peeled off from the master mold and drilled to make the pre-designed flow. Drilled PDMS elements were exposed to oxygen plasma for 30 s and mounted on a clean glass slide (75 mm×25 mm in length×width). The ensemble was then heated again at 80℃ for 30 min for irreversible PDMS-glass bonding. This micro-fabricated chip was connected to a syringe pump (PicoPlus, Harvard Apparatus) with a silicone tube and a 3-way stopcock to integrate a microfluidic chip.

1.3 Antibody immobilization

For antibody immobilization, the microfluidic chip surface was coupled with an amino group layer[31]. Briefly, 2% APTES in 95% acetone was injected into the microchannel and incubated at room temperature for 20 min. After being rinsed with acetone to remove un-reacted silane and dried with nitrogen, the microchannel was introduced by anti-CD59 or anti-BSA mAbs which are pre-mixed with NHS and EDC at a final concentration of 100 μg/mL to activate carboxyl groups. Being incubated at room temperature for 2 h, the activated mAbs were able to covalently bind onto the microfluidic chip surface. After washing un-reacted mAbs out with PBS using a syringe pump, the microchannel was then incubated respectively with 2% BSA or 1.5% casein for 1 h for anti-CD59 or anti-BSA mAb-immobilized microchannel, to block the potential non-specific adsorptions when antigen-expressed or -coupled cells flowed over the chip surface.

1.4 BSA coupling onto RBCs and site density determination

A previously described modified chromium chloride ($CrCl_3$) method was used to couple BSA onto the surface of fresh human RBCs[3,4,27–29]. Briefly, BSA proteins were coupled onto the surfaces of RBCs at different densities using various concentrations of a $CrCl_3$ solution in 0.02 mol/L acetate buffer (pH 5.5). The coupling efficiency of BSA was tested by FACS, using CD58 which is expressed on RBCs at a known density as a standard[32]. To measure site densities of coupled BSA or CD59, RBCs were incubated directly with FITC-conjugated goat anti-mouse antibody at a concentration of 10 μg/mL in 200 μL of FACS buffer (RPMI1640 5 mmol/L EDTA, 1% BSA, 0.02% sodium azide) on ice for 40 min. After washing, the cells were analyzed by FACS. Site densities were then calculated by comparing the fluorescence intensities of the cells with those of standard beads (Bangs Labs, Fishers, IN)[3,28,29].

1.5 System set-up and experimental procedures

Microfluidic system consists of a microfluidic chip, an image grabbing unit, data acquisition and analysis software, as well as a supporting base (Figure 1). In the microfluidic chip, an antibody-immobilized microfluidic
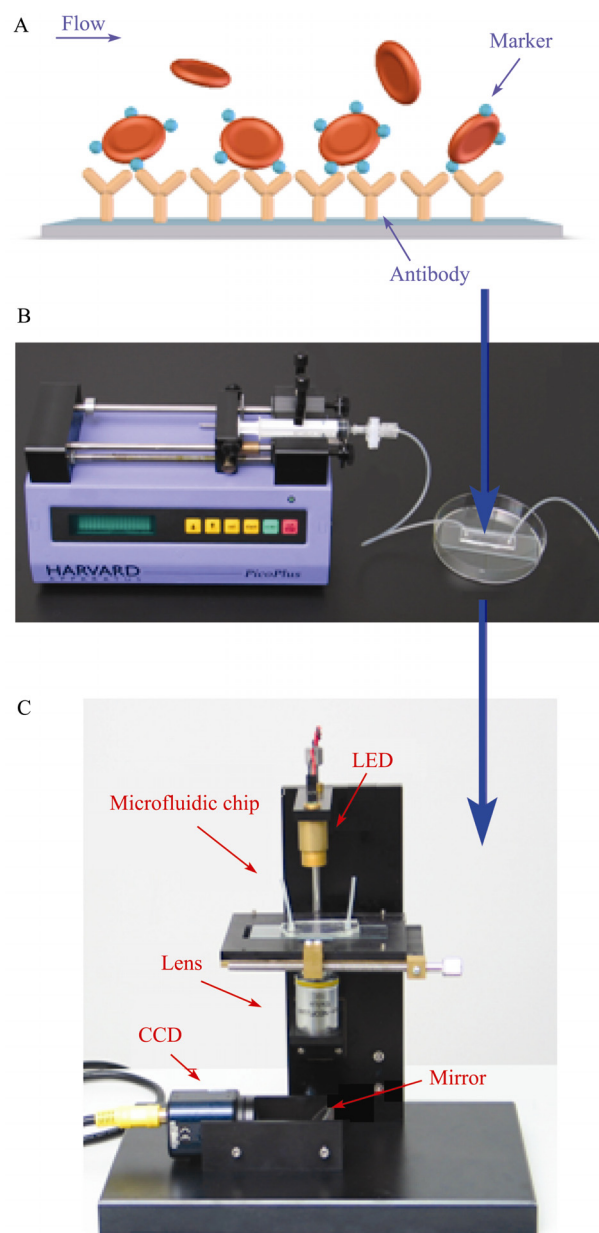

Figure 1 Microfluidic-based system. A, Binding of marker-expressed or coupled cells to an antibody- or ligand-immobilized surface. Driven flow was applied to remove unbound cells from the chip surface. B, Micro-fabricated PDMS microfluidic chip connected to a syringe pump. C, System assembly by integrating a microfluidic chip, a LED lamp with a thin convex, objective, reflecting mirror, and a CCD camera set in a supporting base.

chip (Figure 1A) was placed onto the stage and connected to a syringe pump. The stage was manipulated in three-dimensions to reach the focal plane using a purpose-built displacement controller (Figure 1B). In the image grabbing unit, a LED lamp (4000—10000 mcd) with a convex lens, an objective (10×, Zeiss, Germany), a reflector mirror, and a CCD camera (Sony, Japan) were aligned in an optical design to monitor in real time the captured RBCs inside the microchannel. The grabbed images were transferred and digitalized into a computer *via* the A/D board. The data acquisition and analysis software was developed in house to quantify the capture kinetics of antigen-coupled RBCs to an antibody-immobilized surface. All the components were integrated into a purpose-built supporting base (Figure 1C).

To measure RBC capture, RBCs in PBS at a given concentration (about 10^7/mL) were introduced into the microchannel at a pre-set flow rate by being withdrawn from the end of a syringe pump. Once RBCs were introduced, the pump was turned off to let RBCs settle down and react with the chip surface for about 5 min. The total cell number, N_0, in five pre-set view fields was counted and averaged. After washing unbound cells out by turning up the pump to re-initiate flow at a low flow for about 1 min, the number of cells remaining adherent, N_1, was counted from same view fields and averaged. Capture efficiency, ϕ, was defined as the fraction of adherent cells, that is, $\phi = N_1/N_0$. All the measurements were repeated in triplicate.

1.6 ELISA-based cell binding assay

A modified protocol previously described[33,34] was used to biotinylate RBCs. Plain or BSA-coupled RBCs were rinsed 3 times and re-suspended at about 2.5×10^7 cells/mL in ice-cold PBS. Collected RBCs were biotinylated by adding Sulfo-NHS-Biotin solution at a final concentration of 1 mg/mL and were incubated at room temperature for 30 min following the manufacturer's modified instruction. RBC suspension was then washed three times in PBS/100 mmol/L glycine to quench and remove excess biotin and re-suspended in PBS for use.

To measure cell binding upon an enzyme-linked immunosorbent assay (ELISA), 25 μL of anti-CD59 mAb at 1—20 μg/mL or anti-BSA mAb at 50 μg/mL were added into a 96-well plate and incubated overnight at 4℃. Antibody-coated wells were washed in PBS and then filled with 100 μL of biotinylated plain or BSA-

coupled RBCs at 3×10^6 cells/mL in each well. After being incubated at room temperature for 30 min, 100 μL of PBS were gently added. The plate was turned over to remove unbound RBCs. 50 μL of horseradish peroxidase streptavidin at 5 μg/mL was immediately added into each well and incubated at room temperature for 30 min. The wells were carefully rinsed and then incubated with substrate-dye buffer (*o*-phenylenediamine dihydrochloride at 0.4 mg/mL in citrate phosphate buffer, pH 5.0, H_2O_2 0.03%) in the dark at room temperature for 20 min. 20 μL of stop solution (2 mol/L H_2SO_4) were added into each well to terminate the reaction. The optical density (*A*) value for each well was measured using an ultraviolet spectrometer at 490 nm. Control experiments were done where only 2% BSA, but not the relevant mAbs was present. All the measurements were repeated at least in triplicate.

2 Results

2.1 Specific capture of RBCs

Capture efficiency, ϕ, was used to quantify the binding kinetics of CD59-expressed or BSA-coupled RBCs to anti-CD59 or anti-BSA mAb-immobilized surfaces. As shown in Figure 2A, CD59-expressed RBCs were captured specifically when CD59 antigens were expressed on RBCs and anti-CD59 mAbs were presented on chip surfaces (■). The capture was abolished when the anti-CD59 mAbs were absent (●) or when CD59-expressed RBCs were pre-incubated by soluble anti-CD59 mAbs at a saturated concentration of 2 μg/mL to block CD59 antigens(△). Similar captures were obtained when both BSA proteins and anti-BSA mAbs were present but abrogated when plain RBCs interacted with an anti-BSA mAb-immobilized chip surface (Figure 3B). The resulting capture efficiency, ϕ^N, for non-specific binding was subtracted from total binding, ϕ^T, which returned the net capture efficiency, $\phi^S (=\phi^T - \phi^N)$.

2.2 Effect of flow rate on capture efficiency

Cell capture efficiency was manipulated by flow rate. To test the effect of flow rate, shear flow used to wash unbound cells out was systematically varied at 2, 4, 6, 8, 10, and 12 μL/min at a given cell concentration of 3×10^7 cells/mL. As exemplified in Figure 2A, the total capture efficiency, ϕ^T, for CD59-expressed RBCs exhibited a reduced transition phase when the flow rate was en-

hanced (■). The results were straightforward because higher applied force exerted on CD-59-anti-CD59 bonds *via* RBC surfaces at the higher flow rate shortened the bond lifetime, which in turn accelerated the detachment of bound RBCs. It was also observed that, at a given flow rate, most bound RBCs were still captured firmly regardless of deformation (data not shown). By contrast, a reduced transition phase with flow rate was also obtained at a much lower level of ϕ^N for capturing CD59-expressed RBCs to BSA-blocked surfaces (●) or CD59-expressed RBCs pre-blocked with soluble anti-CD59 mAbs to anti-CD59 mAb-immobilized surfaces (△), further suggesting that RBC capture mediated by antigen-antibody interactions. These results suggested that this antibody-coated chip identified cell-surface markers

Figure 2 Dependence of flow rate and cell concentration. A, Total capture efficiency was plotted against flow rate for capture of CD59-expressed RBCs onto an anti-CD59 mAb-immobilized surface (■), onto a 2% BSA-immobilized surface (●), and for CD59-expressed RBCs pre-incubated with soluble anti-CD59 mAb and then captured onto an anti-CD59 mAb-immobilized surface (△). Data are presented as the mean ± standard deviation (SD) of capture efficiency at least in triplicate. B, total capture efficiency was plotted against cell concentration for BSA-coupled RBCs in both individual (□) and averaged (■) capture efficiencies. Error bars are SD of the mean in quadruplicate.

and the measured capture efficiency varied with the flow rate used.

2.3 Effect of cell concentration on capture efficiency

Cell capture efficiency was also regulated by cell concentration. To conduct the measurements, the concentration of CD59-expressed BRCs was systematically varied at 3×10^5, 3×10^6, 3×10^7, and 1×10^8 cells/mL at a pre-set flow rate of 6 μL/min. As shown in Figure 2B, the total capture efficiency, ϕ^T, for CD59-expressed RBCs exhibited an increased transition phase when the cell concentration increased followed by a steady phase when it reached equilibrium (■). Repeated measurements indicated that the measured capture efficiency exhibited a scattered distribution at a low concentration of 3×10^5 cells/mL but more uniform distributions at the higher concentrations of 3×10^6 or 3×10^7 cells/mL (□). This was because more RBCs were geometrically available to be captured on the chip surface at the higher concentrations. The total capture efficiency, ϕ^T, was lowered at the highest concentration of 1×10^8 cells/mL, presumably due to strong steric repulsion of RBCs away from the chip surface. Thus, an optimal cell concentration of 3×10^7 cells/mL was used to maximize capture efficiency in the following measurements.

2.4 Effect of molecular concentration or density on capture efficiency

Cell capture efficiency was further quantified by antibody concentration or antigen site density. To test this, the concentration of anti-CD59 mAbs was systematically varied at 1, 5, 7, 10 and 20 μg/mL to immobilize the antibody onto the chip surface. As shown in Fig. 3*a*, total capture efficiency, ϕ^T, for CD59-expressed RBCs was reduced at a pre-set flow rate of 6 μL/min and a given cell concentration of 3×10^7 cells/mL when the antibody concentration decreased. At a high concentration (≥5 μg/mL), net capture efficiency was measurable because it was significantly higher than that for non-specific capture (solid bars). At a low (1 μg/mL) or even lower concentration, it was hard to isolate specific capture from total capture of RBCs (open bar). Higher site density on the chip surface was obtained when incubating the antibody at a higher concentration, which formed more antigen-antibody bonds to enhance cell capture efficiency. To further test this, the site densities of BSA were systematically varied at 18, 27, and 45
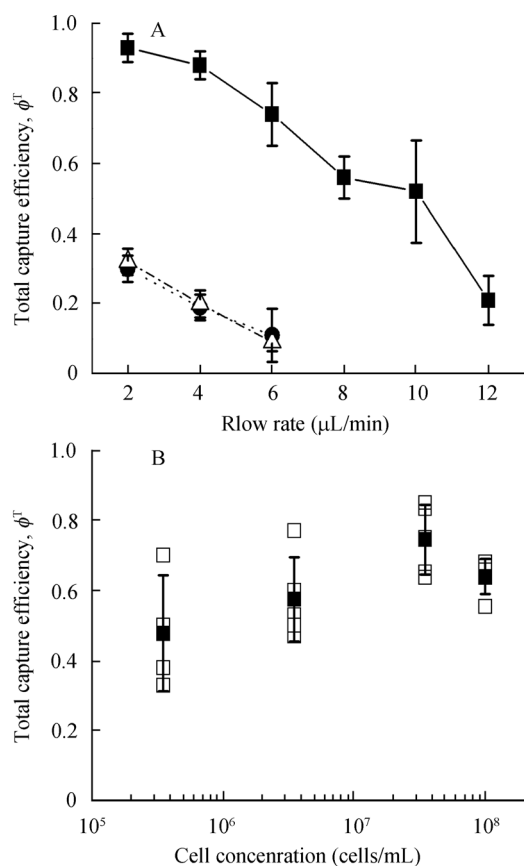
μm^{-2} by varying $CrCl_3$ concentration (Figure 3B)[4,27]. Cell capture efficiency measurements were then done using the same procedures as above. As shown in Figure 3B, total capture efficiency, ϕ^T, for BSA-coupled RBCs exhibited a transition phase when site density increased and a steady phase when it reached equilibrium (■), following the mass transportation law. Also included in Figure 3B was a non-specific capture for plain RBCs to demonstrate significant low capture efficiency at zero site density (□). The data indicated that the cell capture efficiency measured depended on the site densities of surface-bound antigen (or receptors) and antibody (or ligands). These results also promoted the potential for this system to track time-dependent marker expression.
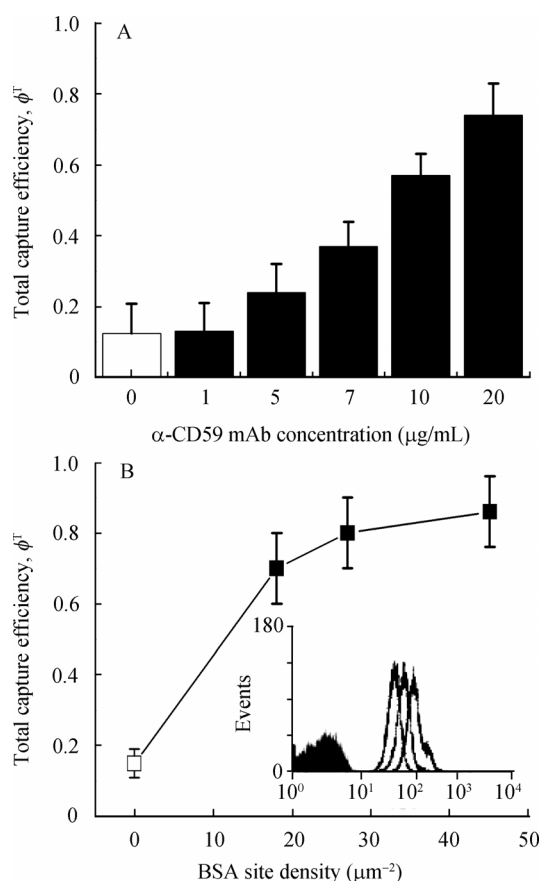

Figure 3 Dependence of antibody concentration and molecular site density. A, Total capture efficiency was plotted against the concentration of anti-CD59 mAbs (solid bars) and 2% BSA proteins (open bar) immobilized onto a chip surface for capturing CD59-expressed RBCs. Data was presented as the mean±SD of capture efficiency at least in triplicate. B, Total capture efficiency was plotted against BSA site density for capturing BSA-coupled (■) and plain RBCs (□) onto an anti-BSA mAb- immobilized surface. Data was presented as the mean±SD of capture efficiency at least in triplicate. Insert represented measured fluorescence intensities for RBCs coupled with BSA proteins at different site densities (open bars) as well as for plain RBCs (close bar).

This is physiologically significant as marker expression on the cell surface varies in different differentiation states and pathological processes[35].

2.5 Comparison to ELISA-based cell binding assay

The microfluidic-based system developed in the current work was further validated in comparison with conventional techniques used in laboratories. As an example, an ELISA-based cell binding assay was modified to measure cell capture efficiency in a 96-well plate. To do that, a calibration curve between the A value and the cell number was first obtained by systematically varying the cell numbers of 2.5×10^4, 5×10^4, 10^5, 2.5×10^5, and 5×10^5. As shown in Figure 4A, the measured A value was linearly proportional to the cell number used (■). Fitting the data with a straight line returned a calibration curve (line) following $y = 2.6 \times 10^{-6} \times N$ ($R^2 = 0.99$) where y and N respectively denoted the A value and cell number.

To measure the capture efficiency from the ELISA-based cell binding assay, 100 μL of CD59-expressed or BSA-coupled RBCs at a given concentration of 3×10^6 cells/mL (which reads $N_0 = 3 \times 10^5$ cells) was added into wells immobilized with anti-CD59 or anti-BSA mAb at the same antibody concentrations or with comparable site densities to those used in a microfluidic-based system (Figure 3A and B). Here three site densities of BSA at 3, 22, and 43 μm^{-2} were used for an ELISA- based cell binding assay, as it is difficult to exactly match site densities when using $CrCl_3$ to couple BSA. After incubation at room temperature for 30 min and washing unbound cells out, bound cells were tested using the ELISA assay, and the measured A value was translated, using the above calibration curve, to the number of bound cells, i.e., N_1. As shown in Figure 4 B and C, net capture efficiencies, ϕ^S, measured from the microfluidic-based system (■) were in strong agreement with those from the ELISA-based cell binding assay (●). It was also evident that higher capture efficiencies were obtained from the microfluidic-based system at high antibody concentrations (> 10 $\mu g/mL$) or site densities (> 15 μm^{-2}), suggesting the higher sensitivity of measurements in the microfluidic-based assay. These results demonstrated the feasibility and reliability of a developed microfluidic-based system for identifying cell-surface markers.

3 Discussion

The goal of the current work was to establish a micro-

fluidic-based system to quantify capture efficiency of bound cells mediated by surface marker-counterpart molecule interactions. Microfabrication techniques were integrated with the microfluidic chip, image grabbing, and data acquisition and analysis (Figure 1). Biological measurements and quantitative tests indicated that the system developed was robust and reliable (Figures 2—4). The advantage of the system was that it provided a well-controlled experimental procedure, automatic data acquisition, and quantitative data analysis using labeling-free samples.

Potential applications for using immobilized antibodies to identify specifically cell-surface marker molecules for phenotyping or for disease diagnosis was first proposed over twenty years ago[36]. In the current work, we developed a novel microfluidic-based system to rapidly determine surface markers. Technically, developing a commercially-available microfluidic-based system requires further investigation. For example, multiple microchannels must be fabricated into a single chip surface to simultaneously identify multiple marker molecules. The autofocus-available image grabbing unit needs to be further developed to optimize cell capture monitoring. A database of the surface marker spectrum is necessary for correlating marker expression with pathological diseases. Nevertheless, our design and measurements provide a basic idea for recognizing marker molecules in a well controlled procedure. As compared with conventional ELISA-based cell binding assay, our results indicated that the antibody-immobilized microfluidic chip consumed less samples and reagents, and presented higher sensitivity and capture efficiency at an intentionally-adjusted flow rate (Figure 4), regardless of the differences in the procedure between the two assays. Automatic washing using a controlled flow in a micro-fluidic system was also advantageous to reduce the uncertainty of the measured optical density value due to manual washing of the ELISA assay[25].

Marker molecules expressed on the cell surface are crucial in clinical diagnosis and prognosis. For example, the expression of the prostate specific membrane antigen (PSMA) is recognized as a representative signal related to prostate cancer[4,28]. Capture efficiency of antigen- or receptor-expressed cells onto an antibody- or ligand- immobilized chip surface is not only governed by the intrinsic binding kinetics of the interacting molecular pair, but is also regulated by such extrinsic factors as flow rate and duration, cell concentration, pro-

tein site densities, as well as fluid mechanics in a microchannel. While the binding kinetics of surface-bound
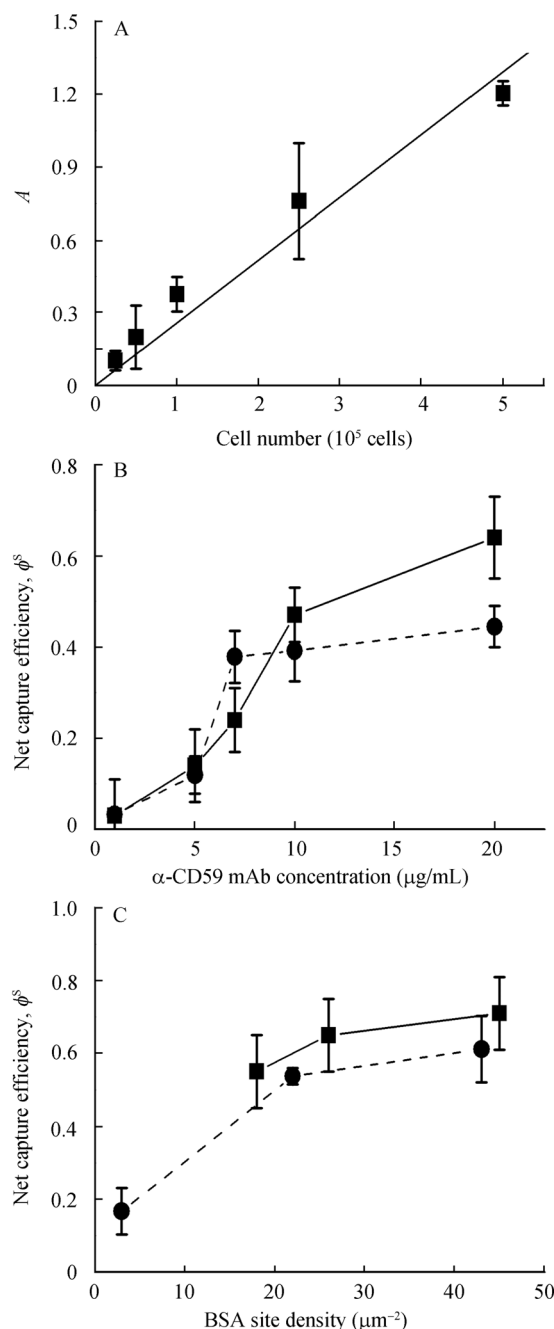

Figure 4 Comparison with ELISA-based cell binding assay. A, A at 490 nm was plotted against cell number. Data was presented as the mean±SD of A value at least in duplicate (■). A straight line was used to fit the data (line). B, Net capture efficiency was plotted against the concentration of anti-CD59 mAbs immobilized onto the chip surface for capturing CD59-expressed RBCs using a microfluidic-based assay (■) and an ELISA-based cell binding assay (●). Data was presented as the mean±SD of capture efficiency at least in triplicate. C, Net capture efficiency was plotted against BSA site density for capture BSA-coupled RBCs onto an anti-BSA mAb-immobilized surface using a microfluidic-based assay (■) and an ELISA-based cell binding assay (●). Data was presented as the mean±SD of capture efficiency at least in triplicate.

molecules have been extensively investigated in previous work[3,4,28,29], which is beyond the scope of the current work, quantitative tests on extrinsic factors were done systematically. Our results suggested that optimized flow rate, cell concentration, antibody concentration and site density were all required to effectively identify marker expression(Figures 2 and 3). Those optimized factors may vary from molecule identities mainly due to the different intrinsic binding kinetics of the interacting molecules. In the current work, two molecular systems were used: one is a typical marker molecule (CD59 antigen), and the other is a representative of artificially- reconstructed proteins (BSA). Further tests for multiple marker molecules on a cell, the same molecules on different cells, as well as time-dependent molecule expressions in different physical-chemical and physio-patho- logical environments are required to promote the clinical applications of the system. To provide mechanistic insights into understanding cell capture on a probe-immobilized substrate, further investigations are required to quantify the impact of cell-cell interactions along the flow, to demonstrate the influence of flow shear on cell capture efficiency near the substrate, and to correlate cell capture efficiency with the kinetic parameters of interacting molecules.

4 Conclusion

We developed a conceptual framework for a microfluidic-based approach to identifying cell surface markers. A prototype, mainly consisting of a microfluidic chip, an image grabbing unit, and data acquisition and analysis software, enabled the quantification of the capture efficiency of antigen- or receptor-expressed cells to an antibody- or ligand-immobilized substrate with robust and reliable measurements. This approach provides some new insights into monitoring cell surface markers in biological studies and in clinical diagnosis and prognosis.

1   Yamada K M. Cell surface marker for malignancy. Nature, 1978, 273: 335—336[DOI]

2   Warnke R A, Link M P. Identification and significance of cell markers in leukemia and lymphoma. Annu Rev Med, 1983, 34: 117—131[DOI]

3   Long M, Zhao H, Huang K S, et al. Kinetic measurements of cell surface E-selectin/carbohydrate ligand interactions. Ann Biomed Eng, 2001, 29: 935—946[DOI]

4   Huang J, Chen J, Chesla S E, et al. Quantifying the effects of molecular orientation and length on two-dimensional receptor-ligand binding kinetics. J Biol Chem, 2004, 279: 44915—44923[DOI]

5   Yang X Y, Chen E, Jiang H, et al. Development of a quantitative cell-based ELISA, for a humanized anti-IL-2/IL-15 receptor beta antibody (HuMikbeta(1)), and correlation with functional activity using an antigen-transfected murine cell line. J Immunol Methods, 2006, 311: 71—80[DOI]

6   Belov L, de la Vega O, dos Remedios C G, et al. Immunophenotyping of leukemias using a cluster of differentiation antibody microarray. Cancer Res, 2001, 61: 4483—4489

7   Belov, L, Huang, P, Barber, N, et al. Identification of repertoires of surface antigens on leukemias using an antibody microarray. Proteomics, 2003, 3: 2147—2154.[DOI]

8   Campbell C J, O'Looney N, Chong Kwan M, et al. Cell interaction microarray for blood phenotyping. Anal Chem, 2006, 78: 1930—1938[DOI]

9   Ko I K, Kato K, Iwata H. Antibody microarray for correlating cell phenotype with surface marker. Biomaterials, 2005, 26: 687—696[DOI]

10 Woolfson A, Stebbing J, Tom B D M, et al. Conservation of unique cell-surface CD antigen mosaics in HIV-1-infected individuals. Blood, 2005, 106: 1003—1007[DOI]

11 Zhu H, Snyder M. Protein chip technology. Curr Opin Chem Biol, 2003, 7: 55—63[DOI]

12 Casciano D A, Woodcock J. Empowering microarrays in the regulatory setting. Nat Biotechnol, 2006, 24: 1103[DOI]

13 Kling J. Moving diagnostics from the bench to the bedside. Nat Biotechnol, 2006, 24: 891—893[DOI]

14 Whitesides G M. The origins and the future of microfluidics. Nature, 2006, 442: 368—373[DOI]

15 Mitchell P. Microfluidics--downsizing large-scale biology. Nat Biotechnol, 2001, 19: 717—721[DOI]

16 Bange A, Halsall H B, Heineman W R. Microfluidic immunosensor systems. Biosens Bioelectron, 2005, 20: 2488—2503[DOI]

17 Bernard A, Michel B, Delamarche E. Micromosaic immunoassays. Anal Chem, 2001, 73: 8—12[DOI]

18 Eteshola E, Balberg M. Microfluidic ELISA: on-chip fluorescence imaging. Biomed Microdevices, 2004, 6: 7—9[DOI]

19 Jiang X, Ng J M, Stroock A D, et al. A miniaturized, parallel, serially diluted immunoassay for analyzing multiple antigens. J Am Chem Soc, 2003, 125: 5294—5295[DOI]

20 Lai S, Wang S, Luo J, et al. Design of a compact disk-like microfluidic platform for enzyme-linked immunosorbent assay. Anal Chem, 2004, 76: 1832—1837[DOI]

21 Mao H, Yang T, Cremer P S. Design and characterization of immobilized enzymes in microfluidic systems. Anal Chem, 2002, 74: 379—385[DOI]

22 Lin C C, Chen A, Lin C H. Microfluidic cell counter/sorter utilizing

multiple particle tracing technique and optically switching approach. Biomed Microdevices, 2008, 10: 55—63[DOI]

23 Wolff A, Perch-Nielsen I R, Larsen U D, et al. Integrating advanced functionality in a microfabricated high-throughput fluorescent-activated cell sorter. Lab Chip, 2003, 3: 22—27[DOI]

24 Du Z, Colls N, Cheng K H, et al. Microfluidic-based diagnostics for cervical cancer cells. Biosens Bioelectron, 2006, 21: 1991—1995[DOI]

25 Liu W T, Zhu L, Qin Q W, et al. Microfluidic device as a new platform for immunofluorescent detection of viruses. Lab Chip, 2005, 5: 1327—1330[DOI]

26 Davies A, Lachmann P J. Membrane defence against complement lysis: the structure and biological properties of CD59. Immunol Res, 1993, 12: 258—275[DOI]

27 Kofler R, Wick G. Some methodologic aspects of the chromium chloride method for coupling antigen to erythrocytes. J Immunol Methods, 1977, 16: 201—209[DOI]

28 Chesla S E, Selvaraj P, Zhu C. Measuring two-dimensional receptor-ligand binding kinetics by micropipette. Biophys J, 1998, 75: 1553—1572[DOI]

29 Wu L, Xiao B, Jia X, et al. Impact of carrier stiffness and microtopology on two-dimensional kinetics of P-selectin and P-selectin glycoprotein ligand-1 (PSGL-1) interactions. J Biol Chem, 2007, 282: 9846—9854[DOI]

30 Duffy D C, McDonald J C, Schueller O J A, et al. Rapid prototyping of microfluidic systems in Poly(dimethylsiloxane). Anal Chem, 1998, 70: 4974—4984[DOI]

31 Zhang Z L, Crozatier C, Le Berre M, et al. In situ bio-functionalization and cell adhesion in microfluidic devices. Microelectron Eng, 2005, 78-79: 556—562[DOI]

32 Selvaraj P, Plunkett M L, Dustin M, et al. The T lymphocyte glycoprotein CD2 binds the cell surface ligand LFA-3. Nature, 1987, 326: 400—403[DOI]

33 Ali M K, Bergson C. Elevated intracellular calcium triggers recruitment of the receptor cross-talk accessory protein calcyon to the plasma membrane. J Biol Chem, 2003, 278: 51654—51663[DOI]

34 Borroto A, Ruiz-Paz S, de la Torre T V, et al. Impaired trafficking and activation of tumor necrosis factor-alpha-converting enzyme in cell mutants defective in protein ectodomain shedding. J Biol Chem, 2003, 278: 25933—25939[DOI]

35 Freedman A S. Cell surface antigens in leukemias and lymphomas. Cancer Invest, 1996, 14: 252—276[DOI]

36 Chang T W. Binding of cells to matrixes of distinct antibodies coated on solid surface. J Immunol Methods, 1983, 65: 217—223[DOI]